A Novel Modeling method of Indoor Broadband Fixed Wireless Access MIMO Ricean Channel Based on Indoor Measurement at 4.9 GHz

Shiwei Hu, Jianhua Zhang, Yu Zhang, Xin Nie
Key Laboratory of Universal Wireless Communications, Ministry of Education
Beijing University of Posts and Telecommunications, Beijing, China

***Abstract*—In this paper, we propose a novel modeling method of indoor broadband fixed wireless access (BFWA) MIMO Ricean channel based on empirical results obtained from stationary channel measurement at 4.9 GHz in both indoor line of sight (LOS) and non-LOS (NLOS) scenarios. The phenomena that K-factors decay versus delay linearly in both the LOS and NLOS scenarios are reported. Extended Saleh-Valenzuela cluster structure is proposed to model Ricean components and has been validated by empirical results. Channel model of IEEE 802.11n is employed as a baseline model and both ergodic and outage mutual information (I) are used as metrics to evaluate the performance of novel method. Simulation results show that, compared to the original way, the performance of novel method on ergodic I and outage I is closer to empirical results in respectively LOS and NLOS scenarios.**

I. INTRODUCTION

Among the last decade, Multiple-Input Multiple-Output (MIMO) systems have been a promising candidate for wireless communications systems [1]. Due to richness of scatters, indoor environment had been thought as an important application scenario of MIMO. Especially, indoor broadband fixed wireless access (BFWA) which is considered as a competitive substitute of traditional wired access methods like DSL, cable modem .etc, is in desperate need of MIMO technologies to improve system throughput. IEEE 802.11n standard was a proposed amendment of previous standards such as 802.11b and 802.11g, with a maximum of 4×4 antenna configuration applied and maximum raw data rate of 600Mbit/s increased from 54 Mbit/s. It has been regarded as a desirable BFWA candidate in office or indoor hotshot scenario [2].

To design and evaluate MIMO technologies, a channel model that can effectively describe the characteristics of realistic wireless channel is very crucial. When channel gain envelope follows Ricean distribution, the shaping parameter namely Riceean K-factor is defined as the ratio of power of time-invariant components (Ricean components) to that of the time-varying components. In the present channel models like ITU-R M.2135 [3], 802.11n [4] .etc, the line of sight (LOS) component is the only Ricean component where the non-LOS (NLOS) components vary with time due to fast fading effect caused by movement of receiver (RX) or transmitter (TX). However, in indoor BFWA system, RX and TX are fixed and the main scatters like walls, ceiling and roof keep static. Intuitively, Ricean components *do not* only consist of LOS component in this kind of environment. Rather than concentrating in the direction and arrival time (delay) of the LOS component, power of Ricean components *disperses* in multiple delays and directions. Based on stationary channel measurements, some similar results have been reported. [5] showed that power ratio of LOS component to NLOS components is smaller than that of Ricean components to time-varying components. In [6], authors also held that Ricean components don't only consist of LOS components in indoor fixed access channels.

As far as the literatures that are known to us are concerned, the phenomenon that Ricean components exist in different delays and the influence of this phenomenon on channel performance have not been mentioned. A channel model that differs from original models which limit K-factor in LOS component is also needed to simulate this kind of channel.

In this paper, a novel modeling method of Ricean components based on the framework of 802.11n channel model [4] is proposed to simulate indoor BFWA channel in either LOS or NLOS scenario. Since the new model of K-factor is independent of applied channel model, this modeling method can be also applied to other channel models. Both ergodic and outage mutual information are used as metrics to judge the performance of proposed modeling method.

The outline of the remaining of the paper is as follows. The channel model and metrics used in this paper are briefly introduced in II. The measurement campaign is described in III. The empirical results and proposed modeling method are presented in VI. Simulation results are reported in V. Section VI concludes the whole paper.

II. CHANNEL MODELS AND METRIC DEFINITION

A. Channel model of IEEE 802.11n standard

The foremost physical layer's improvement of 802.11n compared to previous 802.11 standards(e.g. 802.11a, 802.11g) is the application of MIMO. To evaluate this feature, a MIMO channel model was proposed in [4] and extended Saleh-Valenzuela cluster method is used to simulate the channel spatial characteristics [7]. In one cluster, power of multipath components decays with delay exponentially, and all multipath components share the same power azimuth spectra (PAS). Spatial complex correlation coefficient is derived from

978-1-4244-2515-0/09/$25.00 ©2009 IEEE

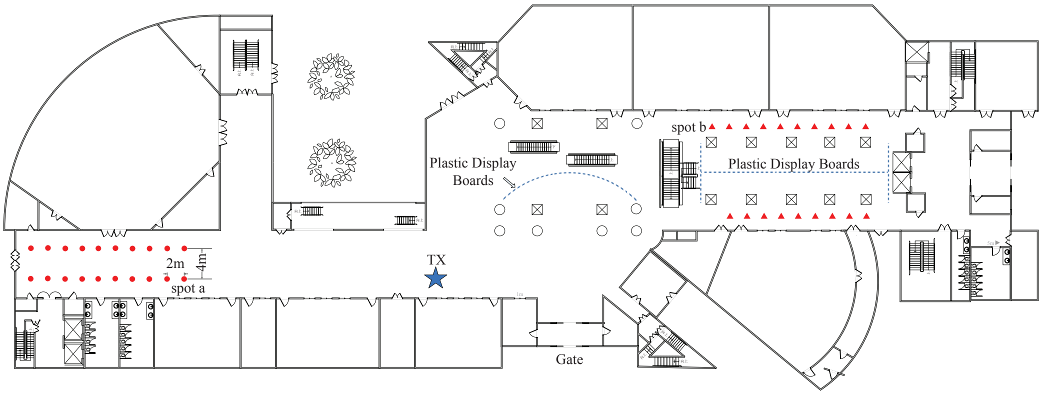

Fig. 1: Layout of measurement scenario. The solid round dots denote the Rx positions of the LOS scenario, and triangles denote the Rx positions of the NLOS scenario. The star denotes the TX position of both the LOS and the NLOS scenarios.

PAS ($P(\phi)$) as

$$R(D) = \int_{-\pi}^{\pi} e^{jD\sin\phi} P(\phi) \mathrm{d}\phi \,, \tag{1}$$

where D is the distance of two antennas, ϕ is either angle of arrival (AOA) or angle of departure (AOD). At delay τ, channel gain matrix can be obtained by using

$$\boldsymbol{H}_{\tau} = \boldsymbol{R}_{\mathrm{r},\tau}^{1/2} \boldsymbol{H}_{\mathrm{w}} \boldsymbol{R}_{\mathrm{t},\tau}^{1/2} \,, \tag{2}$$

where $\boldsymbol{R}_{\mathrm{r},\tau}^{1/2}$ and $\boldsymbol{R}_{\mathrm{t},\tau}^{1/2}$ are the Cholesky decompositions of correlation matrices of RX and TX at delay τ respectively, $\boldsymbol{H}_{\mathrm{w}}$ is the $i.i.d$ standard complex Gaussian random matrix. (2) is also well known as Kronecker model [8].

If Ricean components exist, channel gain matrix $\boldsymbol{H}_{\tau=0}$ should be added with a Ricean matrix which can be expressed as

$$\boldsymbol{H}_{\mathrm{Rice}} = e^{j\varphi} \begin{pmatrix} 1 \\ e^{j\alpha} \\ e^{j2\alpha} \\ \vdots \\ e^{j(N_{\mathrm{r}}-1)\alpha} \end{pmatrix} \left(1, e^{j\beta}, e^{j2\beta}, \cdots, e^{j(N_{\mathrm{t}}-1)\beta}\right) , \tag{3}$$

where φ is the phase of Ricean component, and can be thought uniformly distributed on $(-\pi, \pi]$. $N_{\mathrm{t}}, N_{\mathrm{r}}$ are respectively the elements number of TX and RX. α, β respectively denote the phase difference between adjacent antennas of RX and TX , also can be calculated as

$$\alpha = \frac{2\pi d_{\mathrm{r}} \sin(\theta_{\mathrm{r}})}{\lambda},\ \beta = \frac{2\pi d_{\mathrm{t}} \sin(\theta_{\mathrm{t}})}{\lambda}, \tag{4}$$

d_r, d_t are respectively neighboring antennas spacing of RX and TX. $\theta_{\mathrm{r}}, \theta_{\mathrm{t}}$ respectively denote AOA and AOD. λ is carrier wavelength.

802.11n channel model will be used as a reference model in the following simulations. The chief reasons why selected this model is that this model mainly focuses on the indoor low speed or fixed access channel which is similar to indoor BFWA. Additionally, the extended Saleh-Valenzuela cluster structure of this model can be adopted to model Ricean components.

B. Channel Mutual Information

The channel mutual information ($\mathcal{I}$) is the metric of quantity of information conveyed from channel input to output under a certain input distribution and channel condition [9]. In MIMO system, assuming that the transmitted signal has complex circularly symmetric zero-mean multivariate Gaussian distribution with correlation matrix $(\rho/N_{\mathrm{t}})\boldsymbol{I}_{N_{\mathrm{t}}}$, normalized $\mathcal{I}$ (per unit bandwidth) can be expressed as

$$\mathcal{I} = \log_2 \det \left[\boldsymbol{I}_{N_{\mathrm{r}}} + \frac{\rho}{N_{\mathrm{t}}} \boldsymbol{H}\boldsymbol{H}^{\mathrm{H}} \right] \tag{5}$$

where ρ is the Signal Noise Ratio (SNR).

Ergodic mutual information $\mathcal{I}_{\mathrm{e}} = \mathrm{E}_{\boldsymbol{H}}(\mathcal{I})$ is the average $\mathcal{I}$ under fading channel. Otherwise, outage probability is defined as $p_{\mathrm{out}} = \Pr(\mathcal{I} < \mathcal{I}_o)$, and $\mathcal{I}_o$ is called corresponding outage mutual information. In SISO system, $\mathcal{I}_{\mathrm{o}}$ is mainly affected by distribution of SNR, whereas in MIMO system, $\mathcal{I}_{\mathrm{o}}$ is also influenced by channel spatial characteristics, and the later one is the research interest of this paper.

III. MEASUREMENT CAMPAIGN DESCRIPTION

A. Measurement System

Broadband channel data were collected by the MIMO channel sounder Propsound, which uses the pseudo random binary signal (PRBS) and the time-division multiplexed (TDM). The length of PRBS was 511. The chip rate of PRBS was 100 MHz, which corresponds to 200 MHz RF bandwidth centered around 4.9 GHz. The transmitted power was 16dBm in LOS scenario and 26dBm in NLOS scenario. Both Tx and Rx were equipped with Uniform Linear Array (ULA) with 8 vertical polarized dipole elements. Among the measured data, one snapshot (cycle) refers to the time period separating two consecutive sounding intervals where the same Tx element is active and the same Rx element is scanned, and corresponds to 3-D Channel Impulse Response (CIR) matrix $\boldsymbol{H}_{\mathrm{CIR}}$ with size of $N_{\mathrm{r}} \times N_{\mathrm{t}} \times N_{\tau}$, where N_{τ} is the number of delay taps.

B. Measurement Scenario

Measurements were performed in the first floor of main teaching building at a afternoon of weekday. Students and teachers walked over continually, and Gate and doors switched frequently. Tx and Rx arrays were located at a height of 2.6m and 1.7m above the floor, which is similar to the realistic indoor wireless access systems. Data acquisition were taken at fixed spots as Fig. 1 shows. In the LOS scenario both TX and RX were located in the main corridor with width of 8m. In the NLOS scenario, TX remained the same position as the LOS scenario and RX were located in the other end of the teach building. RX and TX were separated by corner of office room, a stair with one side coved by brick wall, two plastic display boards and some stone columns. There were respectively 20 and 19 spots in LOS scenario and NLOS scenario with a separation of 2m between neighboring spots. In each spot, 400 cycles were collected with the cycle rate of 11.7Hz. The maximal and minimal distance between Rx and Tx are respectively 50m and 25m.

IV. CHANNEL MODELING BASED ON EMPIRICAL RESULTS

In order to get statistic characteristics of broadband channel in delay domain, excess delay is used instead of absolute delay. In the following parts, both terms 'delay' and 'delay tap' refer to excess delay (taps means samples in delay domain). Excess delay is calculated as

$$\tau_{\text{ex}} = \tau_{\text{abs}} - \tau_{\text{abs,1st}}, \tag{6}$$

where τ_{ex} is excess delay and τ_{abs} is the absolute delay. $\tau_{\text{abs,1st}}$ is the absolute delay of first-arrival signal. $\tau_{\text{abs,1st}}$ can be determined by the first delay tap whose power was above a certain threshold. In this paper, as a rule of thumb, this threshold is designated as 15dB below the max power of CIR. This is an empirical value considering that the dynamic range of signal varied from 29dB to 55dB and the maximal power of the noise was about 10dB above the noise floor.

A. *K*-factor

In [10], a simple but effective moment-based method was proposed to estimate narrowband K-factor. It also can be used in broadband case with expression

$$K_\tau = \frac{\sqrt{1-\gamma_\tau}}{1-\sqrt{1-\gamma_\tau}}, \tag{7}$$

where $\gamma_\tau = \text{var}(r_\tau^2)/(\text{E}(r_\tau^2))^2$, and r_τ is the envelope of received signal at delay tap τ. Because K-factor is thought as the function of distance [11], in order to get typical value of K-factor in the LOS/NLOS scenario, K-factors of all spots in the same scenario are averaged.

Fig. 2 illustrates that in the indoor BFWA channel, K-factors was not just confined in the zero-delay tap which corresponds to LOS component. Even though there wasn't a LOS path between RX and TX in the NLOS scenario, K-factors still existed and dispersed in different delay taps. In the both LOS and NLOS scenarios, K-factor decayed with delay.

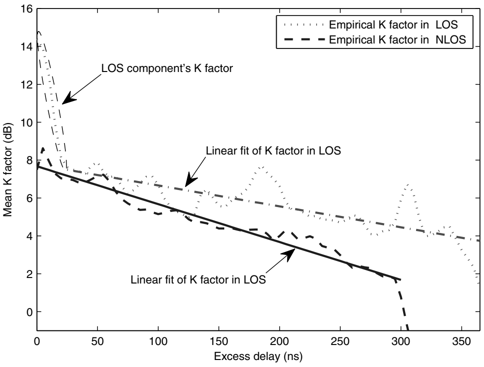

Fig. 2: K-factor varied versus delay

In the LOS scenario, K-factor was significantly large (8dB-14dB) while delay was below 30ns. When delay was greater than 30ns, K-factor kept less than 8dB, and the decreasing trend versus delay can be well fitted by a linear function. As well, K-factor in the NLOS case also can be fitted as a linear function of delay. To include both the LOS and NLOS cases in a unified expression, K-factor can be modeled as

$$K_\tau = \begin{cases} c_1 & \tau = 0 \\ c_2 + c_3\tau & \tau > 0 \end{cases}, \tag{8}$$

where τ is delay measured in nanosecond, K_τ is scaled in dB. c_1, c_2 and c_3 are model parameters. (8) is also able to model K-factor in original method. The c_1, c_2 and c_3 calculated from measurement results are listed in Table. I .

These results are reasonable that K-factor is usually modeled as a linear function of distance between Rx and Tx. It is equivalent that K-factor is a linear function of delay and a linear function of propagation distance. Particularly, in the LOS scenario, when delay was less than 30ns, channel responses were primarily caused by LOS component and multipath components reflected by scatters like corridor walls, ceiling, or floor which are close to LOS path. Propagation conditions of these components were more static compared to the other multipath components which were interacted by farther scatters. Therefore, K-factors of these delay taps were much larger.

On the other hand, K-factor decreased faster versus delay in the NLOS scenario than in the LOS scenario. This can be explained that in the NLOS scenario, multipath components were interacted by more scatters since the NLOS propagation environment was more complicated, whereas in the LOS scenario, multipath components with the same delay were probably bounced by both ends of long corridor and interacted by less scatters.

B. Ricean matrix

Besides K-factor, Ricean matrix ($\boldsymbol{H}_{\text{Rice}}$) modeling is another key issue in MIMO Ricean channel modeling. The original way of modeling MIMO Ricean matrix is conducted in (10) and can be extended to modeling $\boldsymbol{H}_{\text{Rice},\tau}$ at different delay taps. Regarding the $\text{E}(\boldsymbol{H}_{\text{CIR}})$ (averaged over all cycles recorded in a spot) as the broadband 3-D Ricean matrix

($N_\mathrm{r} \times N_\mathrm{t} \times N_\tau$), the AOAs, AODs and delays of Ricean components in LOS spot a and NLOS spot b (marked in Fig. 1) are estimated by Space-Alternating Generalized Expectation maximization (SAGE) algorithm [12] and are illustrated in Fig. 3. Clusters which centered around certain angles and spanned a range of delay are visible and encompassed in Fig. 3. The horizontal lines across the figures plot out the Ricean components with the same delay. It can be observed that, in some delay taps, Ricean components consist of contributions of different clusters. This kind of structure was investigated in extended Saleh-Valenzuela model [7], and had been applied to channel model of 802.11n [4].

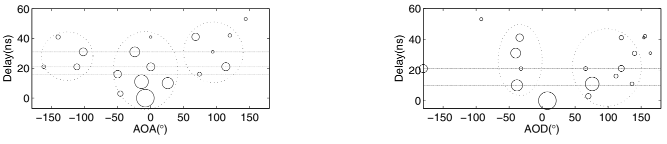

(a) AOA LOS (b) AOD LOS

(c) AOA NLOS (d) AOD NLOS

Fig. 3: SAGE results of Ricean components in spot a and b.

The AOA and AOD of Ricean component at delay tap τ in cluster c are deemed to follow truncated Laplacian distribution which is usually used to model PAS in indoor MIMO channel [3], [4], [7], while the angle distribution and PAS are equivalent to a certain extent. The distribution of Ricean components at delay τ in cluster c writes

$$p_{c,\tau}(\theta) = \frac{Q}{\sqrt{2}\sigma} \exp\left(-\frac{2|\theta - \theta_c|}{\sqrt{2}\sigma}\right) \; -180^\circ < \theta < 180^\circ, \quad (9)$$

where factor Q is used to normalize $Q\int_{-180^\circ}^{180^\circ} p(\theta)\mathrm{d}\theta = 1$. θ_c is the mean value of Laplacian distribution. In the following simulation, θ_c is set as the AOD/AOA of the corresponding cluster in channel model of 802.11n. The parameter σ is the standard deviation of Laplacian distribution and determines the angle separation of Ricean components of different delays in a cluster. Using (3) and AOA and AOD generated by distribution (9) , The Ricean matrix $\boldsymbol{H}_{\mathrm{Rice},c,\tau}$ at delay τ in cluster c can be derived.

Thus, a model based on extended Saleh-Valenzuela cluster structure is proposed to simulate Ricean matrices at different delay taps. In delay tap τ, Ricean matrix is calculated as the superposition of Ricean components in different clusters.

$$\boldsymbol{H}_{\mathrm{Rice},\tau} = \sum_c \alpha_{c,\tau} \boldsymbol{H}_{\mathrm{Rice},c,\tau} \quad (10)$$

where $\alpha_{c,\tau}$ is the square of power of Ricean component at delay tap τ in cluster c. Power of $\boldsymbol{H}_{\mathrm{Rice},\tau}$ equals to 1.

The channel gain matrix at delay τ is obtained by

$$\boldsymbol{H}_\tau = \sqrt{\frac{K_\tau}{1+K_\tau}} \boldsymbol{H}_{\mathrm{Rice},\tau} + \sqrt{\frac{1}{1+K_\tau}} \boldsymbol{H}_{\mathrm{nonRice},\tau}, \quad (11)$$

where $\boldsymbol{H}_{\mathrm{nonRice},\tau}$ is calculated as (2).

V. Simulation Results

A. Settings of simulation

In order to perform simulation with 802.11n channel model, some key parameters were set as follows. Scenario was set to 'D' in LOS scenario and 'E' in NLOS scenario as recommended in [4] as large office environment. Antenna configuration was 8 elements ULA with $\lambda/2$ spacing in both RX and TX side. Carrier frequency was designated as 4.9 GHz. Maximal scatters movement speed was set to 1.2m/s. Effect of fluorescent Lights was removed. Path loss and shadow fading were also ignored to ensure that the average broadband channel coefficients matrices had a uniform power.

$$\mathbf{E}\left(\sum_\tau \mathrm{trace}(\boldsymbol{H}_\tau \boldsymbol{H}_\tau^{\mathrm{H}})\right) = \mathbf{N}_\mathrm{r}\mathbf{N}_\mathrm{t} \quad (12)$$

In LOS scenario, for the sake of comparing proposed model with original model, K-factor of original model is derived to ensure that the power of Ricean components is the same of both models. In original model, Ricean components only distribute in zero-delay tap and LOS direction. In NLOS scenario, there isn't any K-factor and Ricean components in original model. (8) can be applied as a unified model of K-factor. Parameters c_1, c_2, c_3 of different cases are listed in Table. I.

TABLE I: K-FACTOR (dB) MODEL PARAMETERS

	c_1	c_2	c_3
Proposed LOS	14.3	7.77	−0.011
Proposed NLOS	7.67	7.67	−0.020
Original LOS	17.04	−Inf	−Inf
Original NLOS	−Inf	−Inf	−Inf

Parameter estimation based on framework of 802.11n model has not been performed because the assumption of model of Ricean components is inherent in the parameter estimation, and it will lead to unfairness when comparing different Ricean models. Moreover, Deficiencies of Kronecker model get serious when the number of antennas is large [13]. Thus, empirical results are not quite comparable to simulation results to some extent. However, without Precise comparison, the empirical results can still provide a general performance reference of typical indoor BFWA channel.

B. Mutual Information

The cumulative distribution functions (CDF) of mutual information $\mathcal{I}$ of original model and proposed model are illustrated in Fig. 4. Empirical results are also plotted as references. σ which has been defined in (9) is scaled by σ_c which is the corresponding cluster angle spread in 802.11n model (If $\sigma = 0$, Ricean AOA/AOD is deterministic). In LOS scenario, $\mathcal{I}_\mathrm{e}$ of proposed model is larger than that of original model and $\mathcal{I}_\mathrm{e}$ increases when σ gets larger. This result shows that, in proposed model, Ricean components with different

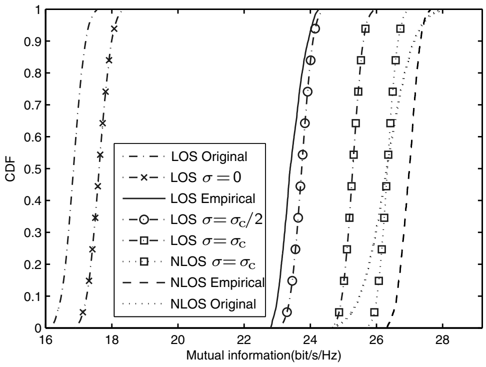

Fig. 4: The mutual information CDF of the proposed model, original models and empirical results in LOS and NLOS scenarios. SNR is fixed to 15dB.

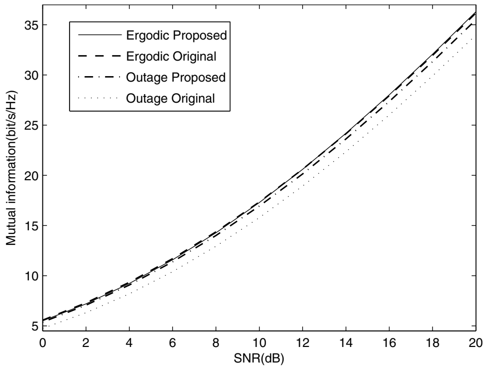

Fig. 5: $\mathcal{I}_\mathrm{e}$ and 1% $\mathcal{I}_\mathrm{o}$ of both original and proposed model under different SNRs

delay taps and directions provide extra degrees of spatial freedom and result in a notable $\mathcal{I}_\mathrm{e}$ increment. Greater angular separation of Ricean components provides more degrees of spatial freedom and leads to larger $\mathcal{I}_\mathrm{e}$. The extra degrees of spatial freedom and the increment of $\mathcal{I}_\mathrm{e}$ are eliminated by original K-factor model since all the power of Ricean component concentrates on the zero-delay tap and unique angle. Comparing the simulation results to empirical results, although not precise, it's still obvious that original model significantly undervalues $\mathcal{I}_\mathrm{e}$ in LOS scenario. On the other hand, σ is a crucial parameter to the proposed model. With a appropriate σ like $\sigma_c/2$, $\mathcal{I}_\mathrm{e}$ of proposed model is close to the $\mathcal{I}_\mathrm{e}$ of empirical result.

In NLOS scenario, with σ=σ_c, the $\mathcal{I}_\mathrm{e}$ of the proposed model (26.33 bit/s/Hz) is rather close to the $\mathcal{I}_\mathrm{e}$ of the original model (26.31 bit/s/Hz). However, standard deviation $\sigma_{\mathcal{I}}$ of $\mathcal{I}$ of the original model (0.633 bit/s/Hz) is much lager than that of either the proposed model (0.242 bit/s/Hz) or empirical results in the NLOS scenario (0.273 bit/s/Hz). Considering $\mathcal{I}_\mathrm{o}$ at a low p_out e.g. 1%, Larger $\sigma_{\mathcal{I}}$ leads to smaller 1% quantile of CDF of $\mathcal{I}$ which corresponds to smaller 1% $\mathcal{I}_\mathrm{o}$. This consequence is validated by Fig. 5 which plots both $\mathcal{I}_\mathrm{e}$ and 1% $\mathcal{I}_\mathrm{o}$ of two models versus different SNR. The curves of $\mathcal{I}_\mathrm{e}$ of both models are rather close, whereas $\mathcal{I}_\mathrm{o}$ of original model is lower than that of proposed model. Taking the comparison of $\sigma_{\mathcal{I}}$ into account, due to lack of Ricean components, the spatial characteristics of original model changes more violently and results in smaller $\mathcal{I}_\mathrm{o}$. By contrast, proposed model has the similar $\sigma_{\mathcal{I}}$ as empirical results and the its $\mathcal{I}_\mathrm{o}$ can be considered to be more reasonable.

VI. CONCLUSION

In this paper, a phenomenon that K-factors decayed linearly with delay in indoor LOS/NLOS BFWA channel is reported. Based on this phenomenon, a novel modeling method of K-factor and Ricean components is proposed based on empirical results obtained from indoor stationary channel measurements. The proposed modeling method shows better agreement with empirical results than original method with metrics of ergodic and outage mutual information. Although the simulation of proposed modeling method is based on channel model of 802.11n, this modeling method of Ricean channel can also be applied to other channel model like ITU-R M.2135 while considering BFWA system.

ACKNOWLEDGMENT

The research was supported in part by National 863 High Technology Research and Development Program of China under Grant No. 2006AA01Z258, and by the Research Institute of China Mobile.

REFERENCES

[1] G. J. Foschini and M. J. Gans, “On limits of wireless communications in a fading environment when using multiple antennas,” *Wireless Personal Communications*, vol. 6, no. 3, pp. 311–335, Mar. 1998.

[2] M. Engels and F. Petre, *Broadband Fixed Wireless Access: A System Perspective*. Springer, August 2006.

[3] “Guidelines for evaluation of radio interface technologies for IMT-Advanced,” REPORT ITU-R M.2135, 2008.

[4] V. Erceg, L. Schumacher, P. Kyrits *et al.*, “TGn Channel Models,” IEEE 802.11-03/940r4, May 2004.

[5] S. Wyne, A. F. Molisch, P. Almers *et al.*, “Outdoor-to-indoor office mimo measurements and analysis at 5.2 Ghz,” *IEEE Trans. Veh. Technol*, vol. 57, no. 3, pp. 1374–1386, May 2008.

[6] A. F. Molisch, L. J. Greenstein, and M. Shafi, “Propagation issues for cognitive radio,” *Proceedings of the IEEE*, vol. 97, no. 5, pp. 787–804, May 2009.

[7] Q. H. Spencer, B. D. Jeffs, M. A. Jensen *et al.*, “Modeling the statistical time and angle of arrival characteristics of an indoor multipath channel,” *IEEE J.Sel. Areas Commun.,*, vol. 18, no. 3, pp. 347–360, Mar 2000.

[8] C. Oestges, “Validity of the kronecker model for mimo correlated channels,” in *Proc. VTC 2006-Spring Vehicular Technology Conference IEEE 63rd*, vol. 6, 7–10 May 2006, pp. 2818–2822.

[9] A. Goldsmith, *Wireless Communications*. Cambridge University Press, August 2005.

[10] L. J. Greenstein, D. G. Michelson, and V. Erceg, “Moment-method estimation of the ricean k-factor,” *Communications Letters, IEEE*, vol. 3, no. 6, pp. 175–176, June 1999.

[11] D. Crosby, V. S. Abhayawardhana, I. J. Wassell *et al.*, “Time variability of the foliated fixed wireless access channel at 3.5 ghz,” in *Proc. VTC 2005-Spring Vehicular Technology Conference 2005 IEEE 61st*, vol. 1, 30 May–1 June 2005, pp. 106–110.

[12] B. H. Fleury, M. Tschudin, R. Heddergott *et al.*, “Channel parameter estimation in mobile radio environments using the SAGE algorithm,” *IEEE J. Select. Areas Commun.*, vol. 17, no. 3, pp. 434–450, March 1999.

[13] M. Ozcelik, N. Czink, and E. Bonek, “What makes a good mimo channel model?” in *Proc. VTC 2005-Spring Vehicular Technology Conference 2005 IEEE 61st*, vol. 1, 30 May–1 June 2005, pp. 156–160.